I-1. PROJECT RESEARCHES

Project 6

PR6 Advancement of integrated system for dose estimation in BNCT

Y. Sakurai

Institute for Integrated Radiation and Nuclear Science, Kyoto University

BACKGROUNDS AND PURPOSES:

Several types of accelerator-based irradiation system for boron neutron capture therapy (BNCT) are under development at present. But, there are a number of subjects, which should be improved for the further advance and generalization of BNCT.

In the viewpoints of medical physics and engineering, the advance for dose estimation is one of the important subjects. For the characterization of irradiation field, quality assurance and quality control (QA/QC), clinical irradiation to actual patient, and so on, an ultimate goal is to perform the three-dimensional and real-time dose estimation in discriminating for thermal, epi-thermal and fast neutron doses, gamma-ray dose, and boron dose, with simplicity and low effort. Considering about this ultimate dose estimation, several kinds of dose estimation method are studied. It is so difficult to realize the ultimate dose estimation using only one method, but it is necessary to use simultaneously more than two methods.

The purposes of this project research are the advance for various dose estimation methods, and the establishment of an integrated system for dose estimation in BNCT.

In the second year of this research project, 2021, the advancement for the respective dose estimation methods were forwarded mainly using Heavy Water Neutron Irradiation Facility (HWNIF) and E-3 Neutron Guide Tube (E-3) at KUR. The integrated system was considered for the simultaneous usage of several dose estimation methods, same as the previous year.

RESEARCH SUBJECTS:

The collaboration and allotted research subjects (ARS) were organized as follows;

ARS-1 (R3P6-1): Establishment of characterization estimation method in BNCT irradiation field using Bonner sphere and ionization chamber (V). (Y. Sakurai, S. Shiraishi, A. Sasaki, N. Matsubayashi, M. Nojiri, R. Narita, H. Kato, D. Fu, T. Takata, H. Tanaka)

ARS-2 (R3P6-2): Study on new type of neutron energy spectrometer for BNCT. (K. Watanabe, Y. Oshima, A. Ishikawa, A. Uritani, S. Yoshihashi, A. Yamazaki, Y. Sakurai)

ARS-3 (R3P6-3): Development and demonstration of Bonner sphere spectrometer for intense neutrons. (A. Masuda, T. Matsumoto, S. Manabe, H. Tanaka, H. Harano, Y. Sakurai, T. Takata)

ARS-4 (R3P6-4): Improvement of the SOF detector system for energy-dependent discrimination and long-term stability. (M. Ishikawa1, S. Ishiguri, H. Handa, K. Baba, K. Takamiya, Y. Sakurai)

ARS-5 (R3P6-5): First direct observation of boron dose distribution with a boron-added liquid scintillator. (A. Nohtomi, H. Maeda, N. Sakamoto, G. Wakabayashi, Y. Sakurai, T. Takata)

ARS-6 (R3P6-6): Development of absolute epi-thermal neutron flux intensity monitor for BNCT (I. Murata, S. Tada, D. Hatano, S. Tamaki, S. Kusaka, H. Tanaka, Y. Sakurai, T. Takada)

ARS-8 (R3P6-8): Study for microdosimetry using silicon-on-insulator microdosimeter in the BNCT irradiation field (V). (Y. Sakurai, N. Ko, T. Takata, H. Tanaka, T. L. Tran, J. Davis, S. Guatelli, A. Rozenfeld, N. Kondo, M. Suzuki)

ARS-10 (R3P6-10): Measurement of BNCT beam component fluence with multi imaging plate system. (K. Tanaka, Y. Sakurai, C. Hatori, T. Kajimoto, H. Tanaka, T. Takata, G. Bengua, S. Endo)

ARS-11 (R3P6-11): Development of 2D real-time neutron imaging system in the BNCT irradiation field. (S. Uno, T. Koike, K. Miyamoto, R. Hosoya, H.Tanaka)

ARS-12 (R3P6-12): Measurements of neutron fluence and gamma ray distribution using thermoluminescence slabs. (K. Shinsho, M. Tanaka, N. Sugioka, H. Tanaka, T. Takata, G. Wakabayashi, W. Chang, Y. Koba)

ARS-14 (R3P6-14): Development and evaluation of 3D gel dosimeter for the measurement of dose distribution in BNCT. (S. Hayashi, Y. Sakurai, M. Suzuki, T. Takata)

ARS-15 (R3P6-15): Establishment of beam-quality estimation method in BNCT irradiation field using dual phantom technique (V). (Y. Sakurai, N. Kondo, D. Fu, T. Takata, H. Tanaka, M. Suzuki)

ARS-16 (R3P6-16): Development of real-time thermal neutron monitor for BNCT. (H. Tanaka, N. Matsubayashi, S. Kurosawa, T. Takata, Y. Sakurai)

ARS-17 (R3P6-17): Quantitative measurement of 478 keV prompt gamma-rays of boron-neutron capture reaction with the ETCC. (T. Mizumoto, S. Komura, Y. Sakurai, T. Takata, T. Tanimori, A. Takada)

ARS-19 (R3P6-19): Evaluation of neutron irradiation fields for semiconductor device irradiation. (H. Tanaka, N. Matsubayashi, T. Takata, Y. Sakurai)

ARS-20 (R3P6-20): Optimization of bolus shape for boron neutron capture therapy - examination using simple shaped phantom for experimental verification -. (T. Takata, H. Tanaka, A. Sasaki, N. Matsubayashi, M. Nojiri, Y. Sakurai, M. Suzuki)

ARS-22 (R3P6-22): Annealing properties of boric acid infused PVA-GTA-I gel irradiated with neutrons. (H. Yasuda, JE. Taño, CAB. Gonzales, Y. Sakurai)

ARS-23 (R3P6-23): Three dimensional model for pre-clinical assessments in BNCT. (K. Igawa, A. Sasaki, K. Izumi, E. Naito, M. Suzuki, N. Kondo, Y. Sakurai)

ARS-7, ARS-9, ARS-13, ARS-18 and ARS-21 could not be performed because of the influence of COVID-19 infection.

PR6-1 Establishment of characterization estimation method in BNCT irradiation field using Bonner sphere and ionization chamber (V)

Y. Sakurai, S. Shiraishi[1], A. Sasaki[1], N. Matsubayashi[1], M. Nojiri[1], R. Narita[1], H. Kato[1], D. Fu[1], T. Takata and H. Tanaka

Institute for Integrated Radiation and Nuclear Science, Kyoto University
[1]Graduate School of Engineering, Kyoto University

INTRODUCTION: Development in accelerator-based irradiation systems for BNCT is underway. In the near future, BNCT using these newly developed systems may be carried out at multiple facilities across the world. Considering this situation, it is important that the estimations for dose quantity and quality are performed consistently among several irradiation fields, and that the equivalency of BNCT is guaranteed, within and across BNCT systems. Then, we are establishing QA/QC system for BNCT.
As part of the QA/QC system, we are developing estimation method for neutron energy spectrum using Bonner sphere [1]. For our spectrometer using Bonner sphere, liquid such as pure water and/or boric acid solution is used as the moderator. A multi-layer concentric-sphere case with several sphere shells is prepared. The moderator and its diameter are changeable without entering the irradiation room, by the remote supply and drainage of liquid moderator in the several layers. For the detector, activation foils are remotely changed, or online measurement is performed using SOF detector, etc.
In 2021, the prototype Remote-changeable Bonner-sphere Spectrometer (RBS) was revised. An experiment was performed for the characteristic verification of the prototype RBS at Heavy Water Neutron Irradiation Facility of Kyoto University Reactor (KUR-HWNIF) [2].
MATERIALS AND METHODS: In the neutron energy spectrometry by Bonner-sphere, the combinations of the moderator material and diameter should be previously decided and prepared. Of course, the more information can be obtained as the more moderators and detectors are prepared. However, the information number from those measured data is less than the combination number, because of the overlapped regions among the combinations. The selection is important, in which the more information number is obtained for the combination number.
The combination of moderator and detector is decided, for that the response functions cannot be approximated by the linear functions of the other response functions. The accuracy and precision for the spectrometry can be higher, because the independent information can be obtained from the measurement by the respective combinations. We were developed the selection method, High Independence Selection (HIS) [3].
On the assumption of the application in the standard epi-thermal neutron irradiation mode of KUR-HWNIF, the combination of the moderators for boron-10 concentration and diameter was optimized by HIS. Based on this optimization, the prototype RBS was revised. Some experiments were performed for the characteristic verification of the revised prototype RBS at KUR-HWNIF.
RESULTS: The configuration of the revised RBS was decided as follows. A five-layer concentric spherical acrylic shell is used as a container. Each acrylic wall is 1 mm in thickness. The moderator injection part is 9 mm in thickness for each layer. Pure water and 0.12-wt% boric acid water for boron-10 were used as liquid moderators. Gold wire was used as the detectors. Figure 1. shows the revised prototype RBS.
Unfolding was performed by GRAVEL using the response function of each Bonner sphere corrected by multiplying the ratio for measured/calculated values. The nominal spectrum of the epi-thermal neutron irradiation mode was input as an initial guess.
The comparison between the nominal spectrum and unfolded spectrum was performed. The spectrum obtained by the unfolding reproduced the nominal spectrum relatively well, but the absolute value was overestimated almost one and a half times.
The accuracy of the revised prototype RBS was improved compared with the first prototype RBS. However, the overestimation was not resolved. It is considered that the possible reasons for the overestimation are the differences in sizes between the actually prepared spectrometer, field size, beam directionality, etc..
CONCLUSION: We have the plans to perform (1) the further revision of the prototype RBS and (2) the preparation of a Bonner sphere spectrometer including the remote mechanism for the supply and drainage of the liquid moderators.

Figure 1. The revised prototype RBS.

REFERENCES:
[1] S. Shiraishi *et al.*, Appl. Radiat. Isot. **163** (2020) 109213.
[2] Y. Sakurai and T. Kobayashi, Nucl. Instr. Meth. A **453** (2000) 569-596.
[3] H. Ueda, Doctoral Thesis (2016).

PR6-2 Study on New Type of Neutron Energy Spectrometer for BNCT

K. Watababe, Y. Oshima, A. Ishikawa[1], A. Uritani[1], S. Yoshihashi[1], A. Yamazaki[1] and Y. Sakurai[2]

Graduate School of Engineering, Kyushu University
[1] Graduate School of Engineering, Nagoya University
[2] Institute for Integrated Radiation and Nuclear Science, Kyoto University

INTRODUCTION: Boron neutron capture therapy (BNCT) is one of the radiotherapies. This is a combined modality of radiotherapy and chemotherapy for cancer treatment. In the BNCT, a boron-containing agent, which is concentrated into tumor cells, are irradiated with thermal neutrons and $^{10}B(n,a)$ reactions are induced. The BNCT is radiotherapy using neutrons. Recently, an accelerator-driven neutron source has actively been developed instead of nuclear reactors, owing to its simplicity of management. The energy spectrum of neutrons, which is irradiated to patients, should be evaluated in order to assure safety of patients.

The conventional technique for neutron spectrometry is the Bonner sphere method. The similar concept is the liquid moderator type neutron spectrometer, in which a small neutron detector can be moved and various neutron responses can be acquired. In this study, we are developing a new neutron detector using an optical fiber. So far, in order to realize the optical fiber type neutron detector showing a neutron peak in the pulse height spectrum, bright neutron scintillators, such as Eu:$LiCaAlF_6$ or LiF/Eu:CaF_2 eutectics, have been used [1]. Recently, we attempted to replace them with the faster Li glass scintillator[2]. For the both cases, we have never controlled a shape of scintillators because the scintillator size have been too small. Since they had random shapes, the Monte-Carlo simulation based study was difficult to be conducted. In order to evaluate the accurate detector response, the scintillator shape is required to be controlled.

We proposed that a transparent composite Li glass scintillator, in which fine Li glass scintillator powder and resin are mixed. This type of scintillator is expected to be easily shaped because it is a resin-based material. In this study, we fabricate the transparent composite Li glass scintillator and evaluate its response to thermal neutron irradiation.

EXPERIMENTS: We fabricated the transparent composite Li glass scintillator. First, a Li glass scintillator was crushed and grinded in a mortar. And then, fine powder of the Li glass and UV curable resin were mixed. We prepared two types of transparent composite scintillator with different mixing ratio. One of them has the mixing ratio of the UV resin to Li glass powder of 1:2 in weight percent. Other one has the ratio of 2:5. Finally, the mixed resin was irradiated with UV light to solidify the resin. Figure 1 shows a photograph of the fabricated transparent composite Li glass scintillator. They were semi-transparent. A small piece of the fabricated transparent composite Li glass scintillator was mounted at a photocathode of a photomultiplier tube(PMT). The scintillator and PMT were shielded with a black sheet against an ambient light. The signal of the PMT was fed into the digital multichannel analyzer, in which the signal pulse height spectrum was created.

Fig. 1 Photograph of the fabricated transparent composite Li glass scintillator.

RESULTS: Figure 2 shows signal pulse height spectra obtained when the fabricated transparent composite Li glass scintillators were irradiated with thermal neutrons. The neutron source was a Cf-252 source surrounded with a polyethylene moderator. The fabricated transparent composite Li glass scintillator shows a clear neutron peak in the signal pulse height spectrum. The peak pulse height was smaller than that of the bulk Li glass scintillator. There is no difference between the composite scintillators with the different mixing ratio.

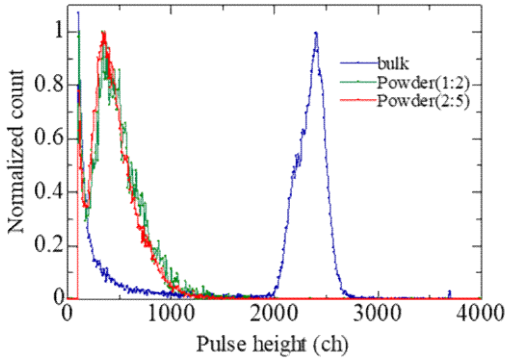

Fig. 2 Signal pulse height spectra obtained when the fabricated transparent composite Li glass scintillator was irradiated with thermal neutrons. The pulse height spectrum obtained by a bulk Li glass scintillator was also plotted.

REFERENCES:

[1] K. Watanabe *et al.*, Nuclear Instruments and Methods in Physics Research Section A , **802**, 1 (2015).
[2] A. Ishikawa *et al.*, Sensors and Materials, **32**, 1489-1495 (2020).

PR6-3 Development and demonstration of Bonner sphere spectrometer for intense neutrons

A. Masuda, T. Matsumoto, S. Manabe, H. Tanaka[1], H. Harano, Y. Sakurai[1] and T. Takata[1]

National Metrology Institute of Japan, National Institute of Advanced Industrial Science and Technology
[1]Institute for Integrated Radiation and Nuclear Science, Kyoto University

INTRODUCTION: Spectrometers for intense neutrons are desired to ensure the performance and safety of boron neutron capture therapy (BNCT). Unfolding method using Bonner sphere spectrometer (BSS) is one of the effective solutions [1]. In this study, two types of Bonner sphere detectors were developed in AIST and demonstrative measurements were carried out at the KURNS.

EXPERIMENTS: Two types of BSS were irradiated by the standard mixed neutron in the heavy water irradiation facility of the KUR [2], as shown in Fig. 1.
The first Bonner sphere detectors consist of HDPE moderators and a pair of lithium-glass scintillators, the GS20 and the GS30, coupled with current-integration-operated PMTs [3] [4].

The second ones consist of HDPE moderators and a spherical ^{3}He proportional counter surrounded by a ^{6}LiF-loaded neutron absorber. Since the ^{6}LiF-loaded layer reduces moderated thermal neutrons just around the thermal neutron detector, detection efficiency is reduced, and the relative response characteristic is not so different from that of the ordinary Bonner sphere detector without the ^{6}LiF-loaded layer.

Fig. 1. BSS with a pair of lithium-glass scintillators (left) and BSS with a ^{6}LiF-shielded ^{3}He proportional counter (right).

RESULTS: Fig. 2 shows results of the measurements using the scintillator-based BSS. Output values are within the operating range of the system. Net neutron-induced current is derived by subtracting the GS30 current from the GS20 current without correction factors, because the correction factors have not been evaluated for used detectors yet. The results will be corrected using the correction factors [3] and neutron spectral fluence will be derived by the Bonner unfolding method [1].

Fig.3 shows output pulse-height spectra from the BSS with the ^{6}LiF-loaded layer. The extent of the pile up was limited within the allowance. Large sphere shows less neutron signals and more γ-ray signals, which resulting from the neutron capture on hydrogen. The results show that the sensitivity-reduced Bonner sphere detector with the ^{6}LiF-loaded layer is acceptable for the BNCT intense neutron beams. Characteristics of the Bonner sphere detectors will be investigated in more detail at AIST and possible combination with neutron detection element will be explored.

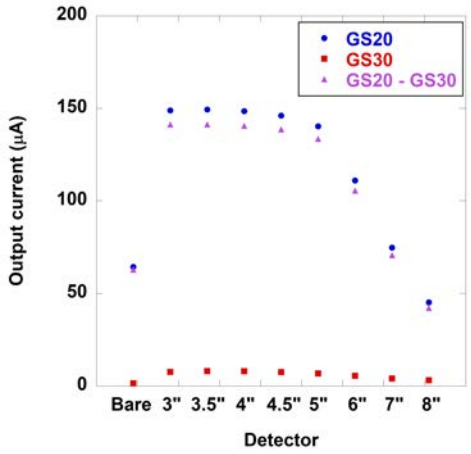

Fig. 2. Measurement results of the scintillator-based BSS.

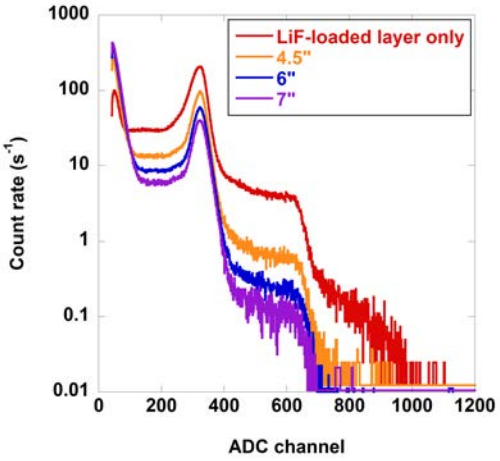

Fig. 3. Pulse height spectra of the BSS with the ^{6}LiF-loaded layer.

REFERENCES:

[1] A. Masuda *et al.*, Appl. Radiat. Isot., **127** (2017) 47-51.
[2] Y. Sakurai and T. Kobayashi, Nucl. Instr. Mes. Phys. Res. A, **453** (2000).
[3] T. Matsumoto *et al.*, Radiat. Prot. Dosim., **188** (2020) 117-122.
[4] A. Masuda *et al.*, 2018 IEEE NSS/MIC Proceedings (2019) 10.1109/NSSMIC.2018.8824697.

This study is supported by Grand-in-Aid for Scientific Research, Japan Society for the Promotion of Science (JSPS KAKENHI Grant Number 19K12638).

PR6-4 Improvement of the SOF detector system for energy-dependent discrimination and long-term stability

M. Ishikawa[1,2], Shu Ishiguri[2], H. Handa[2], K. Baba[2], K. Takamiya[3] and Y. Sakurai[3]

[1]*Faculty of Health Sciences, Hokkaido University*
[2]*Graduate School of Biomedical Science and Engineering, Hokkaido University*
[3]*Institute for Integrated Radiation and Nuclear Science, Kyoto University*

INTRODUCTION: In the conventional BNCT, thermal neutron flux and thermal neutron fluence during treatment could not be measured in real time because gold wire activation was used to evaluate thermal neutron fluence. Therefore, we developed a detector (SOF detector; Scintillator with Optical Fiber Detector) with a plastic scintillator attached to the tip of the optical fiber, tried real-time measurement of thermal neutron flux in neutron capture therapy, and got good results. The long-term stability of the SOF detector and the wide measurement dynamic range (linearity of 10^4 to 10^{10} n/cm^2/s) have been confirmed in previous collaborative experiments. [1,2]
However, signal degradation of SOF detector in long-term exposure was reported [3]. The signal degradation might not be a significant problem in case that calibration can be performed before use. However, signal degradation greatly affects measurement accuracy in case of long-term monitoring because calibration prior to use is difficult. From the previous experiment, it is presumed that the main cause of deterioration of the SOF detector is due to deterioration of the plastic optical fiber, so we tried to conduct two experiments: (A) monitoring deterioration of the SOF probe by using external UV excited signal and (B) the deterioration-accelerated experiment with an SOF detector probe using a quartz optical fiber.

EXPERIMENTS: From the previous experiment, it was presumed that the main cause of deterioration of the SOF detector is due to deterioration of the plastic optical fiber. In order to monitor the SOF probe deterioration, a pulsed UV-LED was used to excite scintillation signals. The decrease of scintillation signals was treated as a comprehensive deterioration including a plastic optical fiber and a scintillator.
Figure 1 shows the deterioration monitoring system using pulsed UV-LED. In addition to the 1-second interval measurement by the SOF detector, the scintillation light excited by the UV-LED was measured once every 10 seconds to assess the deterioration of the SOF probe. Figure 2 shows the SOF signal count rate change during irradiation at the Slant exposure tube with 5 MW. The output of the SOF detector gradually decreases from the start of irradiation and drops to 80% at the end of irradiation. On the other hand, the output of the SOF detector corrected by the measurement by the deterioration monitor system keeps a constant output for 5 hours, indicating that the deterioration correction by the deterioration monitor system is possible.

In addition, as shown in Fig. 3, no deterioration was confirmed in any of the scintillator, the neutron sensitizer (^{6}LiF), and the reflector in the measurement using the quartz fiber.

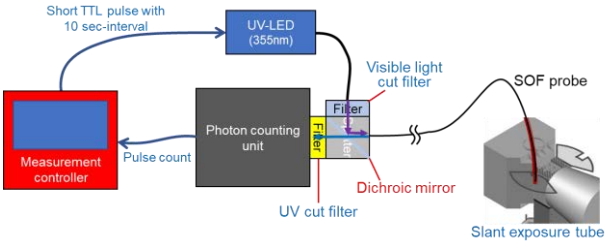

(a) Schematic illustration of deterioration monitor

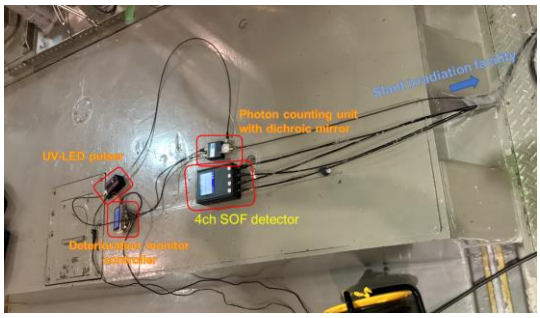

(b) Experimental setup at the Slant exposure tube

Fig. 1. Deterioration monitor using pulsed UV-LED.

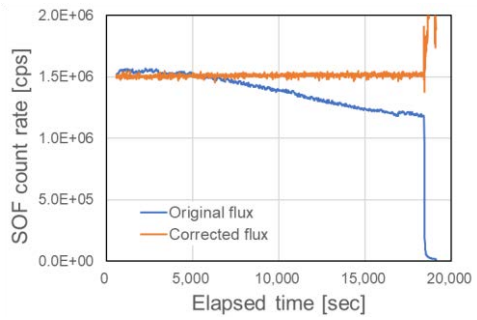

Fig. 2. SOF detector measurement w/ and w/o correction with deterioration monitor system.

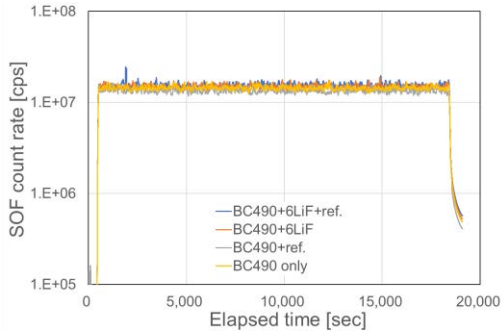

Fig. 3. Deterioration assessment for SOF detector component using a quartz optical fiber.

REFERENCES:

[1] M. Ishikawa *et al.*, Appl. Radiat. Isot., **61** (2004) 775-779.
[2] M. Ishikawa *et al.*, Nucl. Instr. Meth., A **551** (2005) 448-457.
[3] M. Komeda *et al.*, Appl. Radiat. Isot., **67** (2009) 254-257.

PR6-5 First Direct Observation of Boron Dose Distribution with a Boron-added Liquid Scintillator

A. Nohtomi, H. Maeda, N. Sakamoto G. Wakabayashi[1], Y. Sakurai[2] and T. Takata[2]

Graduate School of Medicine, Kyushu University
[1]Atomic Energy Research Institute, Kindai University
[2]Institute for Integrated Radiation and Nuclear Science, Kyoto University

INTRODUCTION: For the boron-neutron capture therapy (BNCT), boron dose plays a significant role to kill tumor cells. However, it is very difficult and almost impossible to measure the boron dose distribution directly due to the short ranges of Li and alpha particles in tissue (~ 10 μm) generated by ^{10}B-neutron capture reactions. Instead, the distribution is usually evaluated by calculations with an information of thermal neutron flux. In the present work, direct observation of ^{10}B-neutron capture reactions (so called "boron dose") was carried out by using a boron-added liquid scintillator [1].

EXPERIMENTS: We dissolved trimethyl borate in a commercially-available liquid scintillator (InstaGel Plus) approximately 1 wt% and 0.25 wt% in natural boron concentration. The boron-added liquid scintillator was filled in a quartz bottle phantom and was irradiated by thermal neutrons (~10^5 n/cm^2/s) during 150, 300 and 600 seconds at E-3 irradiation port [2]. Luminescence of the liquid scintillator was observed by a cooled CCD (SBIG, STF8300M) camera during the irradiation in a black box.

RESULTS: As shown in Fig. 1, the luminescence distribution showed a good agreement with that of the energy deposition of Li and alpha particles from ^{10}B-neutron capture reactions calculated by Monte Carlo simulations (PHITS). When trimethyl borate was not dissolved in the liquid scintillator (0 wt%), no visible luminescence was observed even for 600 seconds irradiation. The luminance value recorded by the CCD camera was simply proportional to the irradiation time of thermal neutrons as indicated in Fig. 2.

From the facts mentioned above, it is evident that the observed luminance is originated from Li and alpha particles generated by ^{10}B-neutron capture reactions. This means the luminescence distribution is directly related to so called "boron dose" to liquid scintillator. To the best knowledge of authors, direct optical observation of the boron-dose distribution has not been reported yet experimentally.

This novel technique will be useful for the quality assurance (QA) purposes of BNCT, because instantaneous neutron irradiation may be enough for observation of the actual intense neutron beam of clinical BNCT (~10^9 n/cm^2/s) with less amount of addition of trimethyl borate. A quick check of the boron-dose distribution will be promising instead of the conventional gold-wire activation method which is generally very time-consuming task.

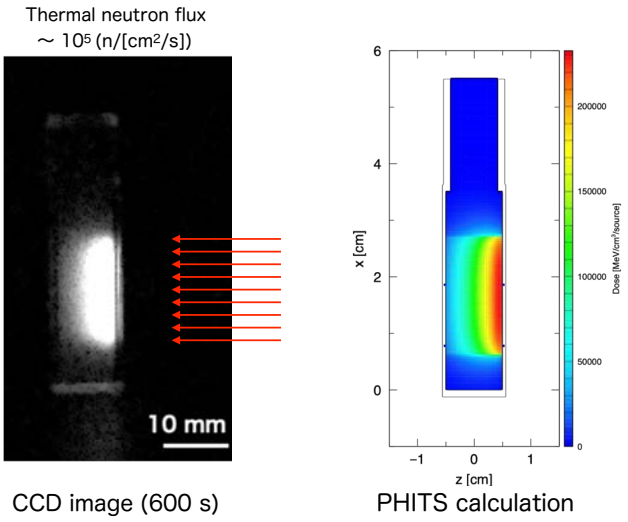

Fi.g. 1 Visualized boron dose distribution observed by a CCD camera (left) and calculated dose distribution deposited by α and Li particles (right).

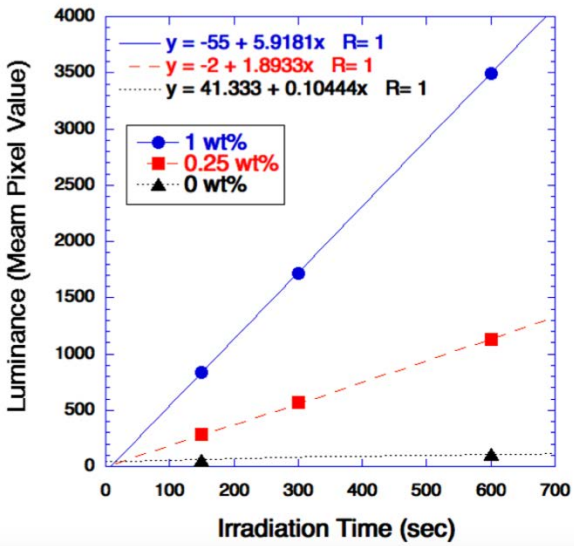

Fi.g. 2 Luminance value of boron-added liquid scintillator as a function of neutron irradiation time.

ACKNOWLEDGEMENT: This work was partially supported by JSPS KAKENHI Grant Number JP19K08202.

REFERENCES:

[1] A. Nohtomi *et al.*, Radiol. Phys. Technol., **15** (2022) 37-44.
[2] T. Kobayashi and, K. Kanda. Nucl. Instrum. Meth., **204** (1983) 525–531.

PR6-6 Development of Absolute Epi-thermal Neutron Flux Intensity Monitor for BNCT

I. Murata, S. Tada, D. Hatano, S. Tamaki, S. Kusaka, H. Tanaka[1], Y. Sakurai[1], T. Takada[1]

Graduate School of Engineering, Osaka University
[1]Institute for Integrated Radiation and Nuclear Science, Kyoto University

INTRODUCTION: BNCT is a promising cancer therapy which kills tumor cells while suppressing exposure dose to normal tissues. Normally, the neutron field of BNCT has an energy distribution spreading within thermal, epi-thermal and fast neutron regions. Because epi-thermal neutrons are generally used for BNCT, we must measure the epi-thermal neutron flux intensity to evaluate the therapeutic effect and patient's exposure dose. In addition, we also have to evaluate the exposure dose of the fast neutrons that may be harmful to the human body. However, it is quite difficult to know such intensities directly and accurately, because there is no suitable neutron spectrometer or no activation material covering epi-thermal or fast neutrons separately. We are therefore developing new monitors to precisely measure the absolute integral flux intensities of epi-thermal (0.5 eV ~ 10 keV), called first monitor, and fast neutrons (10 keV ~ 1 MeV), called second monitor.[1] The objective of this work is to design and develop the two new detectors and to validate them experimentally.

EXPERIMENTS: The first monitor measures the absolute epi-thermal neutron flux intensity from ^{72}Ga activity created via ^{71}Ga(n, γ)^{72}Ga reaction by setting a cubic polyethylene (PE) in which a GaN foil is placed at the center. Fig. 1 shows the sensitivity of the first monitor. For the second monitor, two detectors are used, one of which consists of a cubic PE and a GaN foil covered with a Cd sheet is placed at the center (PE type), and the other one is a similar shape to the first monitor, but with a B_4C sheet surrounding the cubic PE (B_4C type). By making difference of the two ^{72}Ga activities, the absolute fast neutron flux intensity is estimated. Fig. 2 shows the sensitivity of the second monitor. In the present study, the performance of the epi-thermal and fast neutron monitors were verified experimentally at KUR, Kyoto University. Irradiations were carried out for 5 and 15 min. in 5 MW operation for the first and second monitors, respectively.

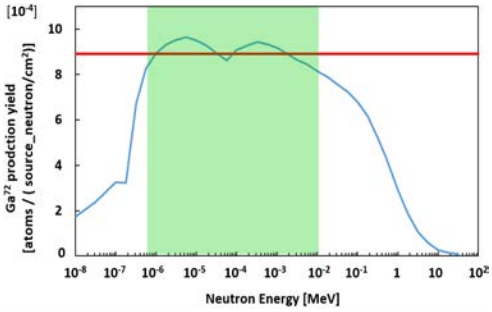

Fig. 1 Sensitivity of the first monitor.

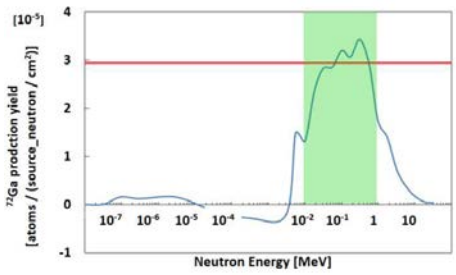

Fig. 2 Sensitivity of the second monitor.

RESULTS: The activities of ^{72}Ga in the monitors were carried out just after their irradiations. The measurements were performed with an HpGe detector. Absolute fluxes were deduced from the obtained activities with the sensitivities shown in Figs. 1 and 2. The results are summarized in Tables 1 and 2. In the tables, the nominal value means the value evaluated at KUR.

Table 1 Absolute epi-thermal neutron flux intensity obtained by the first monitor.

	Experimental value (E)	Nominal value (C)	C/E
^{72}Ga activity [kBq]	(3.31±0.05)x10^3	—	—
ϕ_{epi} [n/cm^2/sec]	(8.67±0.13)x10^8	7.26x10^8	0.84

Table 2 Absolute fast neutron flux intensity obtained by the second monitor.

	Experimental value (E)	Nominal value (C)	C/E
^{72}Ga activity*1 [kBq]	(1.32±0.02)x10^3	—	—
^{72}Ga activity*2 [kBq]	(1.56±0.02)x10^3	—	—
ϕ_{epi} [n/cm^2/sec]	0.6x10^{7} *3	4.94x10^7	7.8

*1 For the PE type detector.
*2 For the B4C type detector.
*3 The estimated error is larger than 100%.

From Table 1, the experimental result of the first monitor is a little larger than the nominal value of KUR. This experimental value was already corrected considering the high energy part of the neutron spectrum. The bare estimation is 5% larger than this value. The first monitor was confirmed to work properly from the present result. On the other hand, as for the second monitor the experimental value shows very small compared to the nominal value. This is due to subtraction of the two activities, namely, as the result the difference is very small and is beyond the statistical errors of the activity measurements. The point is that though the high energy neutron contribution in the neutron spectrum is so small, the sensitivity below 10 keV is not perfectly zero. Now we are modifying the design. Practically, the sensitivity is revised so as to realize zero sensitivity below 10 keV.

REFERENCES:

[1] Y. Kashiwagi *et al.*, "Development of epi-thermal neutron beam intensity detector with ^{71}Ga(n,γ)^{72}Ga reaction for boron neutron capture therapy." *Appl. Radiat. Isot.*, **151**, pp.145-149, 2019.

PR6-7 Study for microdosimetry using silicon-on-insulator microdosimeter in the BNCT irradiation field (V)

Y. Sakurai, N. Ko[1], T. Takata, H. Tanaka, T. L. Tran[1], J. Davis[1], S. Guatelli[1], A. Rozenfeld[1], N. Kondo and M. Suzuki

Institute for Integrated Radiation and Nuclear Science, Kyoto University
[1]Kansai BNCT Medical Center, Osaka Medical College
[2]Centre for Medical Radiation Physics, University of Wollongong

INTRODUCTION: Research and development into several types of accelerator-based irradiation systems for boron neutron capture therapy (BNCT) is underway [1,2]. In the near future, BNCT using these newly developed irradiation systems may be carried out at multiple facilities across the world. In contrast to conventional radiotherapy, the types of radiation present in BNCT consists of many distinct radiation components, each having a different biological weighting factor.
Microdosimetry is an effective dosimetry technique in a mixed radiation environment. Using this technique, it is possible to derive the relative contributions of different radiation modalities. The feasibility study of a novel 3D mesa bridge silicon-on-insulator microdosimeter (SIM) in BNCT [3], developed by University of Wollongong (UOW).
A new-type silicon microdosimeter and its application for boron neutron capture therapy (BNCT) are continuously investigated mainly by Monte Carlo simulation.
MATERIALS AND METHODS: Two detector configurations were investigated, based on the current 3D mushroom microdosimeter. The first structure consists of a cylindrical p+ core electrode through the center of the SV with n+ ring electrode wrapped around the outside of the SV. The second structure consists of a cylindrical n+ core electrode through the center of the SV with p+ ring electrode wrapped around the outside of the SV. Each SV has a diameter and height of 10 μm and the pitch between each individual SV is 40 μm to reduce cross talk between neighboring row of detectors. A total of 2500 individual SVs were connected in an array with odd and even detector row readout channels.
PHITS was used for this study. The T-deposit tally, which scores dose and event-by-event deposition energy distribution was used to calculate the energy deposited inside the SV of the mushroom microdosimeter. The microdosimetric spectrum (frequency mean and dose mean lineal energy distribution) were calculated by dividing the deposited energy by the average chord length of the SV.
The neutron response of the new-type detector were investigated using the neutron source for the mixed neutron irradiation mode of Heavy Water Neutron Irradiation Facility installed in Kyoto University Reactor (KUR-HWNIF) [4].
RESULTS: The ion track of 840 keV Li-7 ions produced inside the p+ region is shown in Figure 1. Similarly, with the alpha particles, higher number of Li-7 ions were deposited inside the SV with the p+ core through the center.
The number of Li-7 depositing it's full energy (840 keV) was also found to be higher with the p+ core design, shown in Figure 2. The range of 840 keV Li-7 ions inside silicon is approximately 2.5 μm. Most of the Li-7 generated inside the p+ core will deposit all its energy inside the SV. However, the Li-7 ions generated inside the p+ ring will only deposit a portion of its energy inside the SV before escaping.
CINCLUSION: It was found that the absorbed dose was approximately 2.4 times more with the p+ core design. No dose was deposited to the surrounding PMMA with the p+ core design.

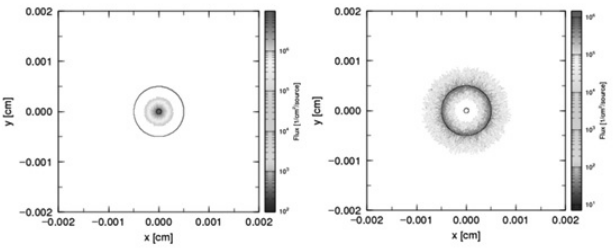

Fig. 1. Ion track of 840 keV Li-7 ions inside a single SV. Left) p+ core through the centre of the SV. Right) p+ ring around the outside of SV.

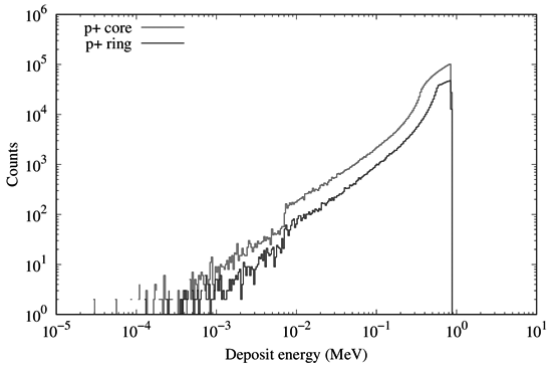

Fig. 2. Deposit energy of 840 keV Li-7 ions inside the SV for p+ core and p+ ring.

REFERENCES:

[1] H. Tanaka *et al.*, Nucl. Instr. Meth. B **267** (2009) 1970-1977.
[2] H. Kumada *et al.*, Appl. Radiat. Isot. **88** (2014) 211-215.
[3] L. T. Tran *et al.*, IEEE Trans. Nucl. Sci. **62** (2015) 3027-3033.
[4] Y. Sakurai and T. Kobayashi, Nucl. Instr. Meth. A **453** (2000) 569-596.

PR6-8 Measurement of BNCT beam component fluence with multi imaging plate system.

Kenichi Tanaka, Yoshinori Sakurai[1], Chiharu Hatori[2], Tsuyoshi Kajimoto[2], Hiroki Tanaka[1], Takushi Takata[1], Gerard Bengua[3], Satoru Endo[2]

Division of Liberal Arts Sciences, Kyoto Pharmaceutical University
[1]Graduate School of Advanced Science and Engineering, Hiroshima University
[2]Institute for Integrated Radiation and Nuclear Science,, Kyoto University
[3]Auckland City Hospital

INTRODUCTION: Measurement of beam fluence spatial distribution is required for quality assurance in the irradiation field for boron neutron capture therapy. This study investigated the use of the multi imaging plate (IP) system which consists of IPs and beam component converters.

EXPERIMENTS: The converter configuration is shown in Fig. 1. The IP is BAS-TR from Fuji Film corporation, Japan. The IP #1 in carbon is to detect gamma rays via secondary electrons, #2 for epithermal neutrons via secondary particles of ^{6}Li(n,α)^{3}H reactions, and #3 for fast neutrons via recoiled protons. Here, material #2 is polyethylene. Material #1 is polyethylene infused with LiF, where ^{6}Li is enriched up to 95 at% The concentration of ^{6}Li in Material #1 is 10 wt%. The details of the converter was described previously [1].
The experiment was performed with the standard epithermal neutron irradiation mode of KUR-HWNIF [2] at 1 MW. The beam size was set to about 120 × 120 mm^2 using the collimator. The irradiation for 2 minutes was performed 3 times..

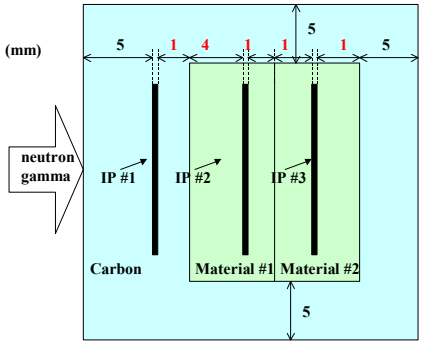

Fig. 1 Converter configuration.
The figure is not in scale.

The fluence ϕ_j of each component was determined using the following model;

$$PSL = \begin{pmatrix} PSL_1 \\ PSL_2 \\ PSL_3 \end{pmatrix} = \begin{pmatrix} a_{11} & a_{12} & a_{13} \\ a_{21} & a_{22} & a_{22} \\ a_{31} & a_{32} & a_{33} \end{pmatrix} \begin{pmatrix} \phi_1 \\ \phi_2 \\ \phi_3 \end{pmatrix} = A \cdot \phi \quad (1),$$

$$\phi = A^{-1} \cdot PSL \quad (2),$$

where a_{ij} denotes the response fuction of the ith IP for the component j estimated by the PHITS simulation [3]

RESULTS: The fluence estimated using the results for the three IPs are shown in Fig. 2. All of three beam components yielded positive values successfully. The reproducibility of the results is about 10-30% in standard deviation. The reduction of the deviation is planned to be investigated.

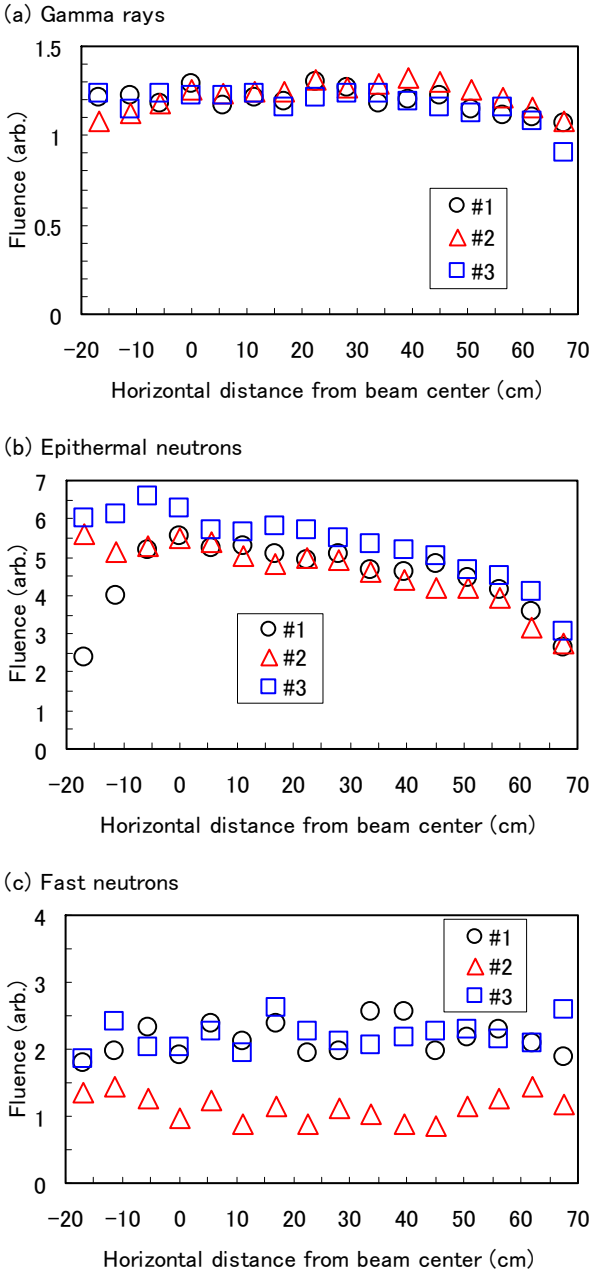

Fig. 1 Estimated fluence distribution.

REFERENCES:

[1] K.Tanaka *et al.* Appl. Rad. Isot. **115** (2016)212-220.
[2] Y.Sakurai and T.Kobayashi *Nucl. Instr. Meth.* **A453** (2000)569-596.
[3] T.Sato *et al.* J. Nucl. Sci. Technol. **50** (2013)913-923.

PR6-9 Development of 2D Real-Time Neutron Imaging System in the BNCT Irradiation Field

S. Uno[1], T. Koike[2], K. Miyamoto[3], R. Hosoya[3] and H.Tanaka[4]
[1] *High Energy Accelerator Research Organization* (*KEK*)
[2] *Faculty of Health Sciences, Kyorin University*
[3] *BeeBeans Technologies Co.Ltd*
[4] *Institute for Integrated Radiation and Nuclear Science, Kyoto University* (*KURNS*)

INTRODUCTION: We have been developing a 2D real-time neutron imaging system using a gas electron multiplier (GEM) [1]. Boron neutron capture therapy (BNCT) is a radiation therapy that selectively destroyed tumor cells by means of high linear energy transfer charged particles released by nuclear reaction caused by thermal neutrons irradiation of ^{10}B. In order to irradiate tumor cells that have taken up ^{10}B efficiently with thermal neutrons, neutron attenuation by the tissue must be taken into account, so an epithermal neutrons irradiation field are required. For the higher accuracy of BNCT, it is important to quality assurance and control of the irradiation field, such as properly evaluate to spatial distribution and fluence rate of the epithermal neutron beams. In this study, the performance of our system were evaluated using E-3 Neutron Guide Tube (E-3) and Heavy Water Neutron Irradiation Facility (HWNIF) of the Kyoto University Research Reactor.

EXPERIMENTS: Our real-time neutron imaging system consists of a detector module (GEM chamber and readout electronics board) and a PC that controls the detector and processing/display the acquisition data [2]. The detector module has a compact size with dimensions, 444mm × 270mm × 41mm. The effective detection area is 100mm × 100mm. These signals are processed by an FPGA-based data acquisition board, and the resulting digitized neutron event data is recorded to PC via Gigabit Ethernet. The GEM chamber works as a gas radiation detector for neutrons by detecting the charged particles emitted through a ^{10}B(n, α)^{7}Li nuclear reaction. It is incorporates a cathode plane coated with a thin layer (0.05μm thickness) of ^{10}B, a single GEM used to amplify the charge deposited in the gas of the detector (Ar-CO_2, 70:30,1atm), and 128 X and 128 Y strips with a 0.8mm pitch strip planes with 2D readout. Detection efficiency for thermal neutrons is 0.2%. Our system have a feature of a spatial resolution of approximately 1 mm (FWHM), an excellent time resolution of 15 ns, low sensitivity to gamma-ray, and Mcps rate capability. The GEM is the double-side printed circuit board, which consists of low temperature co-fired ceramic (LTCC) with 100μm thickness as an insulator and gold layers with 6μm thickness on both sides as an electrode. It has also a large number of holes with 100μm diameter and 200μm pitch (LTCC-GEM) [3]. The LTCC-GEM is quite robust and stability against the large discharge, it is employed to prevent the breakdown of short-circuit between two electrodes of the GEM by abnormal discharge. To evaluate whether this system can image the neutron distribution in real-time, experiments were performed on thermal neutrons at E-3 and epithermal neutrons at HWNIF, and the system response to increased neutron fluence were also evaluated.

RESULTS: Figure 1 shows real-time spatial distribution of the thermal neutron beam, and its beam profiles. From the measurement (FWTM) of the obtained images, the horizontal and vertical lengths were 14.2mm and 20.6mm, respectively. Those are almost consistent with the actual physical dimension of the collimator (beam collimator aperture H: 14mm, V: 18mm), but the horizontal beam profile was asymmetric (at the base), which shows a tendency similar to the result of Nohtomi et al [4]. The thermal neutron fluence rate was estimated to be 0.5× 10^{6}n/cm^{2}s at a reactor output of 1MW. In the future, it will be necessary to compare it with the evaluation of thermal neutron fluence rate by the activation analysis using gold foil.

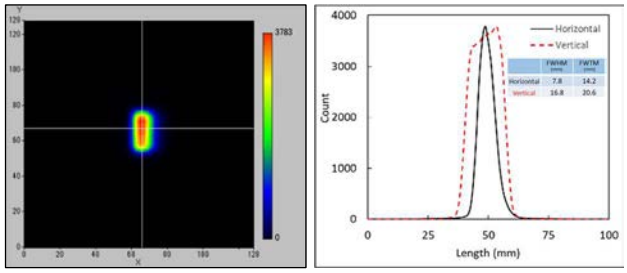

Fig.1. Real-time spatial distribution of the thermal neutron beam, and its beam profiles at E-3.

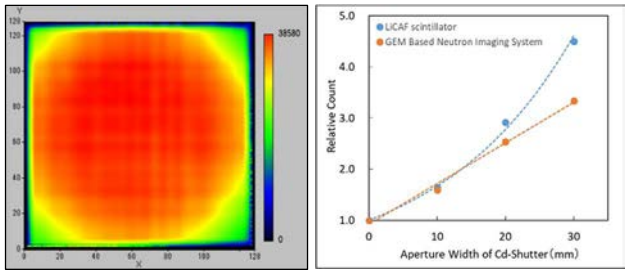

Fig.2. Real-time spatial distribution of the neutron beam and the variation of relative counts on aperture width of Cd-Shutter at HWNIF.

Fig. 2 shows the neutron spatial distribution at the collimator surface at HWNIF. The beam condition of the neutron irradiation field could be evaluated in real-time and the collimator shape could be clearly seen. As a result of changing the aperture width of the Cd-Shutter to increase the neutron fluence, we found that our system showed good counts linearity. It is presumed that the exponential increase in the compared scintillation monitor was due to the location of the detector, and it is necessary to make a more accurate comparison in a similar arrangement.

REFERENCES:

[1] F. Sauli, Nucl. Instrum. Meth. A 386 (1997)531.
[2] S. Uno *et al,* Physics Procedia 26 (2012)142.
[3] K.Komiya *et al,* J. Jpn. Soc. Prec. Eng.84.11 (2018)936.
[4] A.Nohtomi *et al,* KURNS.Prog.Rep.2018 (2019)68.

PR6-10 Measurements of Neutron Fluence and Gamma ray Distribution using Thermoluminescence Slabs

K. Shinsho, M. Tanaka, N. Sugioka, H. Tanaka[1], T. Takata[1], G. Wakabayashi[2], W. Chang, Y. Koba[3]

Graduate School of Human Health Science, Tokyo Metropolitan University

[1] KURNS

[2] Graduate school of Science and Engineering Research, Kindai University

[3]Center for Radiation Protection Knowledge, QST-NIRS

INTRODUCTION: Boron Neutron Capture Therapy (BNCT) is one of the radiation therapies using neutrons and ^{10}B drugs which are attracted to tumors. BNCT is expected to be next-generation cancer therapy which will improve the QOL of patient because it is able to irradiate a cancer cell at the molecular level selectively. However, dosimetry techniques in mixed neutron-gamma fields have not been established yet. Therefore, we focused on neutron and gamma ray measurements using two- dimensional thermoluminescence dosimeter (2D-TLD). The 2D-TLD which we used is thermoluminescence (TL) phosphor Cr doped Al_2O_3 ceramic plate (2-D Al_2O_3: Cr TLD) [1] and BeO ceramics plate.

In this study, we investigated that neutron imaging using 2-D Al_2O_3: Cr TLD and Cd neutron-gamma ray converter technique, and gamma ray dosimetry using BeO ceramics plate in mixed neutron-gamma fields.

EXPERIMENTS:

1. Thermal neutron fluence distribution measurements. Low melting point Al_2O_3 of Chibaceramic MFG Co. LTD., which was composed of Al_2O_3 > 99.5 wt% was used. The bulk density of the plates was 3.7g·cm^{-1}. The dimensions used for the glow curve measurements were 80 × 80 × 0.7 mm^3. The concentration of Cr_2O_3 in the present study was 0.05 wt%. Fig.1 shows the Diagram of neutron imaging using 2-D Al_2O_3: Cr TLD and Cd neutron-gamma ray converter technique. Collimator sizes were 5 mm, 10 mm, and 20 mm. The Two - dimensional TL measurement system consists of a CMOS camera, 80 ×80 mm^2 heater, and a dark box. After exposure, the TL slabs were heated to 400 ℃ for 5 min. The TL images were captured using a CMOS camera equipped with a thermal cut filter.

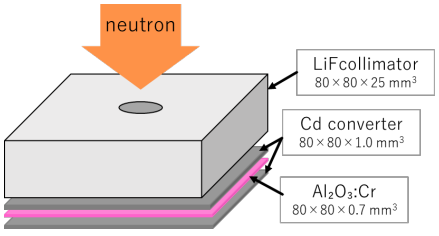

Fig.1 Diagram of neutron imaging using 2-D Al_2O_3: Cr TLD and Cd neutron-gamma ray converter technique.

curve measurements.

2. Gamma ray dosimetry

The BeO ceramic TLD (Thermalox® 995, Materion Corp.) and Na-doped BeO powder TLD (UD-170LS, Panasonic) were used. BeO ceramic TLD content of at least 99.5 wt% and were 10 × 10 × 1.0 mm^3. Na-doped BeO powder TLDs were encapsulated in a ⌀2 mm ×12 mm quartz glass tube. Both TL phosphors were compared to evaluate the usefulness of ceramic BeO for distribution measurement.

In both experiments the irradiation fields are the mixed neutron irradiation mode in KUR-HWNIF, with a power of 1MW.

RESULTS: Figure2 shows the OCR of Al_2O_3: Cr using Cd converter at mixed neutron irradiation mode in KUR-HWNIF. This 2-D Al_2O_3: Cr TLD and Cd neutron-gamma ray converter technique was found to obtain thermal neutron fluence distributions with high spatial resolution. In the future, we will proceed with the verification by theoretical analysis to improve the accuracy of the measurement in the penumbra region.

Figure 3 shows the Gamma ray dose for irradiation time of BeO ceramic TLD and Na-doped BeO powder TLD. The BeO ceramic TLDs showed the same characteristics as Na-doped BeO powder TLDs in the BNCT irradiation field. It was suggested that γ-ray dose distribution measurement is possible by using BeO ceramic, which can be made large area.

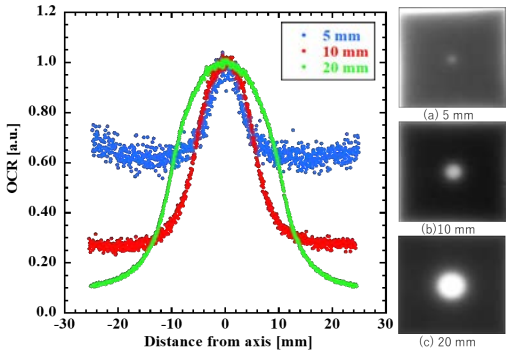

Fig.2 OCR of Al_2O_3: Cr using Cd converter at mixed neutron irradiation mode in KUR-HWNIF.

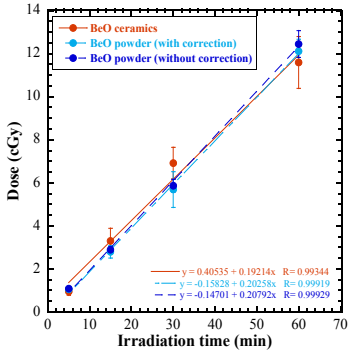

Fig.3 Gamma ray dose for irradiation time of BeO ceramic TLD and Na-doped BeO powder TLD.

REFERENCES: [1] K. Shinsho *et al.*, Sensors and Materials., 30 (2018) 1591-1598

PR6-11 Development and evaluation of 3D gel dosimeter for the measurement of dose distribution in BNCT

S. Hayashi, Y. Sakurai[1], M. Suzuki[1], and T. Takata[1]

Department of Clinical Radiology, Hiroshima International University
[1] Institute for Integrated Radiation and Nuclear Science, Kyoto University

INTRODUCTION: Three-dimensional (3D) gel dosimeters have been developed for the 3D dose measurement of the complex dose distributions in clinical applications [1]. These devices utilize radiation-induced chemical reactions in the gel to preserve information about the radiation dose. The 3D absorbed dose distribution is deduced from the distribution of the reactant measured by imaging modalities, such as MRI (magnetic resonance imaging), X-ray CT (computed tomography), and optical CT. These gel dosimeters have excellent dose properties such as high sensitivity, dose rate independence, and a wide dose range, on X- and gamma-rays and the potential as a 3D dosimeter has been suggested.

In recent years, we have been studying the application of radiochromic gel dosimeters to dose evaluation in neutron irradiation. Up to last year, the optical dose-response of the PVA-I (PVA-GTA-I) radiochromic gel dosimeters [2, 3] on the irradiation of neutron beams with different energy spectra from a nuclear reactor was examined and its availability was investigated. In the results, the significant dose response improved by the addition of the hydrated electron scavenger as a sensitizer was demonstrated while the undesirable dose dependence was also observed.

So, this year, we investigated the dose-response and the potential of another type of radiochromic gel dosimeter that utilizes organic dye, leuco crystal violet (LCV) [4].

EXPERIMENTS: As sensitizers, boric acid, $B(OH)_3$, containing ^{10}B of 20% naturally, were added into the LCV radiochromic gel dosimeter. The concentrations in the gel were 0, 25, and 50 mM of $^{10}B(OH)_3$. The resulting solution was subdivided by pouring into PMMA cuvettes (4.5 mL, 1 cm path length). The neutron irradiations were performed using Heavy Water Neutron Irradiation Facility (HWNIF) of Kyoto University Research Reactor (KUR, power of 1 MW). The samples were irradiated in air at room temperature. The three different modes (thermal neutron rich for 30 min, epi-thermal and fast neutron rich for 50 min, and the mixed modes for 20 min) of neutron beams made by heavy water spectrum shifter and cadmium thermal-neutron filters were applied to the samples. The measurements were performed at room temperature using an UV–Vis spectrophotometer (SHIMADZU, UV-1600PC, Japan). The change in the absorbance (ΔAbs.) at the peak wavelength (600 nm) was investigated as the dose response.

RESULTS: Figures 1(a) and 1(b) show the absorption spectra and the dose responses of the gel samples containing different concentration of boric acid exposed to neutron beam of mix, thermal, epi-thermal and fast modes, respectively.

In the result, the sensitizing effect of ^{10}B was observed as in the gel dosimeter investigated earlier such as PVA-I gel dosimeter. However, its sensitivity was significantly lower than that of the other gel dosimeters. It was suggested that when using the LCV gel dosimeter, it is necessary to add the other sensitizer such as a radical generator.

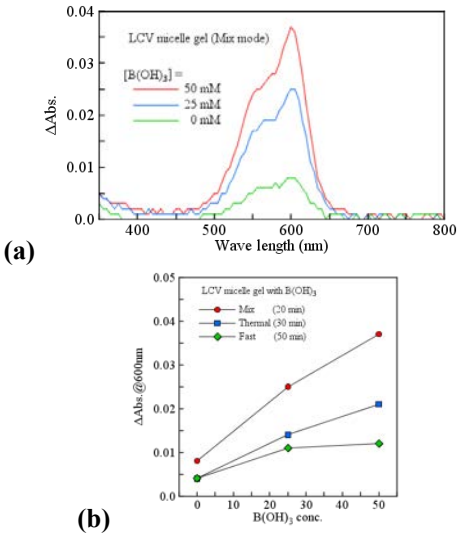

Figure 1 (a) Absorption spectra of the samples containing different concentrations of boric acid irradiated by the mix mode. (b) The dose enhancement with ^{10}B at each mode.

REFERENCES:

[1] M. Marrale and F. d'Errico, *Gels* **7** (2021) 74.
[2] S. Hayashi *et al.*, *Radiat. Meas.* **131** (2020) 106226.
[3] S. Hayashi *et al.*, *J.Phys.; Conf. Ser.* **2167** (2022) 012014.
[4] A. T. Nasr *et al.*, *Phys. Med. Biol.* **60** (2015) 4685-704.

PR6-12 Establishment of beam-quality estimation method in BNCT irradiation field using dual phantom technique (V)

Y. Sakurai, N. Kondo, D. Fu[1], T. Takata, H. Tanaka and M. Suzuki

Institute for Integrated Radiation and Nuclear Science, Kyoto University
[1]Graduate School of Engineering, Kyoto University

INTRODUCTION: Development in several types of accelerator-based irradiation systems for boron neutron capture therapy (BNCT) is underway. Many of these systems are nearing or have started clinical trials. Before the start of treatment with BNCT, the relative biological effectiveness (RBE) for the fast neutrons (over 10 keV) incident to the irradiation field must be estimated.
Measurements of RBE are typically performed by biological experiments with a phantom. Although the dose deposition due to secondary gamma rays is dominant, the relative contributions of thermal neutrons and fast neutrons are virtually equivalent under typical irradiation conditions in a water and/or acrylic phantom. Uniform contributions to the dose deposited from thermal and fast neutrons are based in part on relatively inaccurate dose information for fast neutrons.
The aim of this study is the establishment of accurate beam-quality estimation method mainly for fast neutrons by using two phantoms made of different materials, in which the dose components can be separated according to differences in the interaction cross-sections. The fundamental study of a "dual phantom technique" for measuring the fast neutron component of dose is reported [1].
In 2021, verification experiments for the dual phantom technique were performed using Heavy Water Neutron Irradiation Facility installed in Kyoto University Reactor (KUR-HWNIF) as in the previous year. Biological experiments were performed using the solid phantoms, which were made based on the simulation results.
MATERIALS AND METHODS: One of the dual solid phantoms was made of polyethylene with natural lithium fluoride for 30 weight percent (LiF-polyethylene phantom), and the other phantom was made of polyethylene with 95%-enriched lithium-6 fluoride for 30 weight percent (^{6}LiF-polyethylene phantom).
Glioblastoma U87MG ΔEGFR cells were cultured in Dulbecco Modified Eagle medium (DMEM) with 10 % fetal bovine serum in 5 % CO_2 incubator at 37 ℃. The cells were divided in two groups. One was p-boronophenylalanine (BPA, consisting of ^{10}B) treated group, and the other was non-treated group. The treatment group was cultured with 25 ppm BPA containing medium overnight.
The neutron flux and gamma-ray dose rate were measured using activation foils and thermo-luminescent dosimeter, respectively. The depth dose distributions for the thermal neutron, fast neutron and gamma-ray components were determined based on the simulation calculation results normalized referring to the measured values.
The epi-thermal neutron irradiation mode was used for the phantom experiments.
RESULTS: Figure 1 shows the depth distributions of the cell survival for the BPA administration group, BPA(+), and the non-administration group, BPA(-), in the LiF-polyethylene phantom. The survival rates compared to non-irradiated control was higher in Non-treated cells than those in BPA-treated cells in LiF-polyethylene phantom.
Figure 2 shows the depth distributions of the cell survival in the ^{6}LiF-polyethylene phantom. The survival rates compared to non-irradiated control showed no difference between non-treated cells and BPA-treated cells in ^{6}LiF-polyethylene phantom.
CONCLUSION: The ^{6}LiF-polyethylene phantom absorbs thermal neutrons although it has not significant effect in fast neutron dose. No difference in survival rates between non-treated cells and BPA-treated cells with ^{6}LiF-polyethylene phantom indicated fast neutrons might not effect cell survival. On the other hand, due to mixture of thermal neutron in LiF-polyethylene phantom, BPA-treated cells were killed effectively compared with non-treated cells through n-alpha reactions. In addition, colony forming assays will be performed to confirm the effect of fast neutrons on cell survival.
ACKNOWLEDGMENT: This work was supported by JSPS KAKENHI Grant Number JP 16H05237.

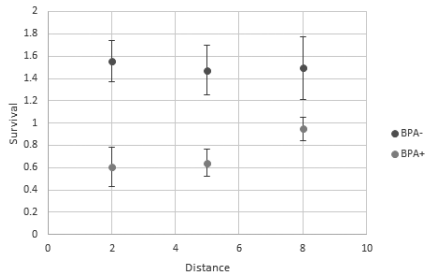

Fig. 1. Depth distributions for the cell survival in the LiF-polyethylene phantom.

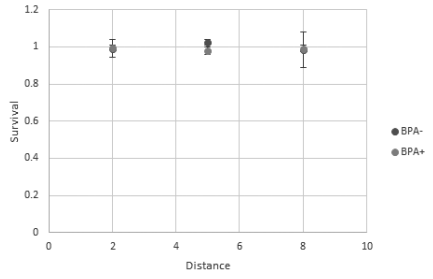

Fig. 2. Depth distributions for the cell survival in the ^{6}LiF-polyethylene phantom.

REFERENCES:
[1] Y. Sakurai *et al.*, Med. Phys. **42** (2015) 6651-6657.

PR6-13 Development of real-time thermal neutron monitor for BNCT

H. Tanaka[1], N. Matsubayashi[1], S. Kurosawa[2], T. Takushi[1], Y. Sakurai[1]

[1]*Institute for Integrated Radiation and Nuclear Science, Kyoto University*
[2]*Institute for Materials Research, Tohoku University*

INTRODUCTION: Treatment of head and neck cancers with the accelerator-based BNCT system is now available at medical institutions [1]. It is necessary to assure the quality of the therapeutic beam before treatment can be performed. Until now, thermal neutron flux has been measured using the activation method that has been used in research reactors. This method does not provide real-time information. In medical institutions, it is desired to perform quality assurance quickly and accurately, and there is an urgent need to develop a real-time thermal neutron detector.

A thermal neutron monitor using a combination of Eu: $LiCaAlF_6$(LiCAF) scintillator and an optical fiber has been developed [2]. However, since LiCAF scintillator have a long decay time, it is important to develop a fast-response scintillator to measure thermal neutron flux in the BNCT irradiation field with a high dynamic range.

In this study, fast-response Cs_2LiYCl(Ce)(CLYC) scintillator crystals were prepared, and neutron irradiation tests were performed in the E-3 guide tube.

EXPERIMENTS: Because CLYC scintillators were deliquescent, the crystals were encapsulated in quartz glass. The crystals were placed in a photomultiplier tube, and the output waveform was obtained with an oscilloscope. The neutron and gamma-ray components can be discriminated based on the relationship between the counts integrated over the entire pulse time (Total : T) and the counts integrated from a certain point after a certain time to the final point of the pulse (Decay component : D).

RESULTS: The relationship between T and 1-D/T is shown in the results in Fig. 1. The data projected in the y-axis direction are also shown in Fig. 2. The two-dimensional plot confirms that the events below about 0.2 are neutron events. On the other hand, the projected figure confirms that the neutrons and γ-rays are sufficiently discriminated.

CONCLUSION: The neutron and gamma-ray discrimination ability of the CLYC scintillator was confirmed in the E-3 guide tube. In the future, we aim to install them in optical fibers and adapt them to the irradiation field of BNCT.

Acknowledgements

We thank Prof. Akira Yoshikawa's laboratory staff of Institute for Materials Research, Tohoku University for their guidance in the fabrication and evaluation of scintillator crystals.

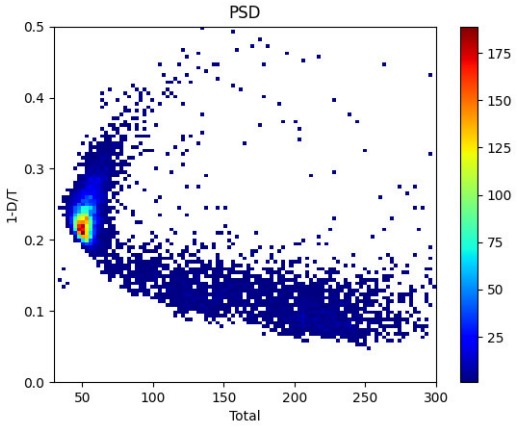

Fig. 1. Relationship between total components and decay components of pulse shape.

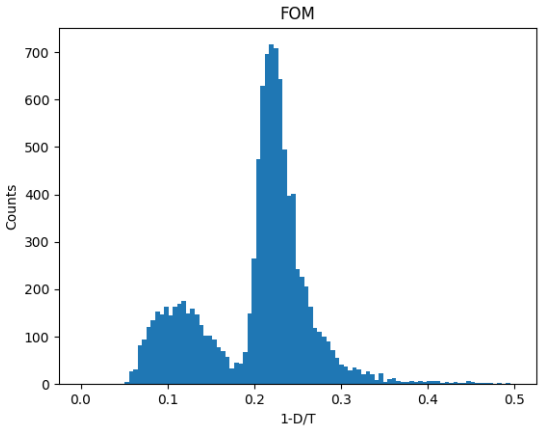

Fig. 2. Pulse shape discrimination of CLYC scintillators.

REFERENCES :

[1] Hirose K., Konno A., Hiratsuka J., Yoshimoto S., Kato T., Ono K., Otsuki N., Hatazawa J., Tanaka H., Takayama K., Wada H., Suzuki M., Sato M., Yamaguchi H., Seto I., Ueki Y., Iketani S., Imai S., Nakamura T., Ono T., Endo H., Azami Y., Kikuchi Y., Murakami M., Takai Y.Boron neutron capture therapy using cyclotron-based epithermal neutron source and borofalan (10B) for recurrent or locally advanced head and neck cancer (JHN002): An open-label phase II trial, Radiotherapy and Oncology, 155, pp. 182 – 187(2021).

[2] Tanaka H., Sakurai Y., Takata T., Watanabe T., Kawabata S., Suzuki M., Masunaga S.-I., Taki K., Akabori K., Watanabe K., Ono K. Note: Development of real-time epithermal neutron detector for boron neutron capture therapy, (2017) Review of Scientific Instruments, 88 (5), art. no. 056101.

PR6-14 Quantitative Measurement of 478 keV Prompt Gamma-rays of Boron-neutron Capture Reaction with the ETCC

T. Mizumoto, S.Komura, Y. Sakurai[1], T. Takata[1], H.Kimura[2], A.Takada[3] and T. Tanimori[3]

Fukushima SiC Applied Engineering Inc.
[1]Institute for Integrated Radiation and Nuclear Science, Kyoto University
[2]Kyoto Pharmaceutical University
[3]Graduate School of Science, Kyoto University

INTRODUCTION: Boron neutron capture therapy (BNCT) is one of the promising cancer treatment methods. However, we have not yet obtained a good monitoring method of the treatment effect in real-time during BNCT. If we get images of 478 keV gamma rays generated by the boron-neutron capture reaction, and measure their intensity and generation positions, we can check the treatment effect on BNCT. As such imaging detector, we have been developing electron tracking Compton cameras (ETCCs). ETCCs are advanced Compton cameras which take the information of the recoil direction of electrons and can uniquely determine the arrival direction of sub-MeV/MeV gamma ray event by event. In the present study, we carried out the following three types of experiments based on previous studies to confirm the performance of our ETCC [1].

EXPERIMENTS AND RESULTS:

Exp. 1: We carried out the prompt gamma-ray imaging tests for a boron containing solution in a 4.5 mm diameter tube which simulates a small tumor tissue. The tube was located just above the ETCC and was irradiated with thermal neutrons at E-3 at the 1-MW operation. This experiment was performed for four tubes with different ^{10}B concentrations (0, 462, 926, 1385 ppm). The experimental setup is shown in Fig. 1. The ETCC measured the prompt gamma rays emitted from the solution during irradiation time. As the result, high quality 478 keV gamma-ray images with a spatial resolution of less than 1 cm. As shown in Fig.1, we also comfirmed that the relationship between the detection rate of 478 keV gamma-rays and B-10 concentrations relatively matches well with simulation result.

Exp. 2: We carried out the prompt gamma-ray imaging studies on U87 MG tumor-bearing mice treated with BPA with neutron irradiation with E-3 neutron beam line at the 5-MW operation. Each mouse was anesthetized and administered 1000 mg/kg of BPA by tail vein injection, then fixed in a plastic case. We carried out the measurement with an ETCC and a mouse placed just above it. We also carried out another measurement of a mouse with two ETCCs installed facing each other. Analysing data of an ETCC, we confirmed that the bright position in the back-projection image of 478 keV gamma-rays shows just the irradiation position of the mouse. The analysis of stereo-ETCC data is in progress.

Exp. 3: We also carried out performance test of the ETCC in a BNCT environment using Heavy Water Neutron Irradiation Facility of KUR at the 1-MW operation. As shown in Fig. 2, we set a 10-cm cubic boron containing solution in the irradiation room. The ETCC measures the 478 keV prompt gamma rays which emit from the solution and pass through the cylindrical hole in the ceiling. This experiment was performed with solution with several B-10 concentrations (0, 46, 93, 230 ppm). We obtained 478 keV gamma-ray backprojection images in which the position of the solution appears brighter. We also obtained that the relationship between the detection rate of 478 keV gamma-rays and ^{10}B concentrations matches well with simulation result.

These results show that the ETCC has the high potential of the quantitative imaging and monitoring of 478 keV prompt gamma-rays of Boron-neutron capture reaction.

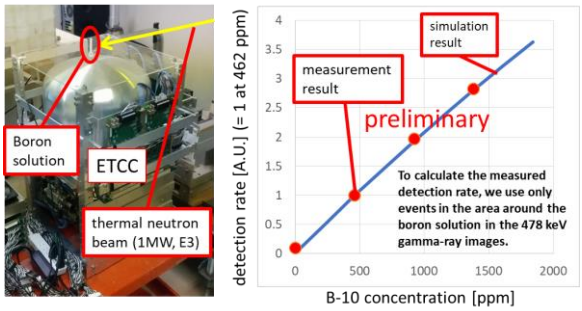

Fig.1 Left: Photograph on Exp.1. Right: The relationship between 478keV gamma-ray detection rate of the ETCC and B-10 concentration of the solution.

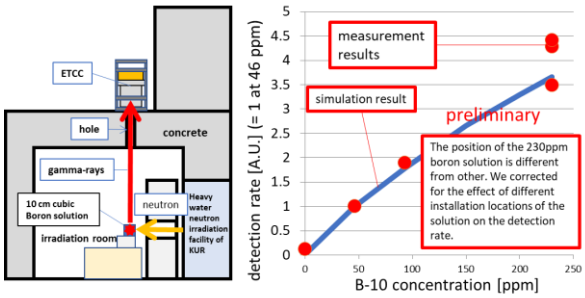

Fig.2 Left: Schematic view on Exp.3. Right: The obtained result of the relationship between 478keV gamma-ray detection rate of the ETCC and B-10 concentration of the solution.

REFERENCES:

[1] S. Komura *et al.*, KURNS Progress Report 2020.

PR6-15 Evaluation of neutron irradiation fields for semiconductor device irradiation

H. Tanaka[1], N. Matsubayashi[1], T. Takushi[1], Y. Sakurai[1]

[1]*Institute for Integrated Radiation and Nuclear Science, Kyoto University*

INTRODUCTION: In the irradiation field of BNCT, electronic devices with semiconductor devices such as neutron monitors, patient monitoring cameras, and implantable pacemakers may be irradiated. If semiconductor devices contain nuclides that have a large capture cross section for thermal neutrons, charged particles are generated in the semiconductor devices when they are irradiated by thermal neutrons. The charged particles generate electron-hole pairs in their trajectories, and this charge becomes a noise current in the semiconductor device. This current can cause semiconductor devices to fail. In addition, semiconductor devices are becoming finer and finer every year, and the signal current is becoming smaller and smaller. In other words, they tend to be more sensitive to noise.

For thermal neutrons, systematic data are lacking [1]. It is also important to investigate the effects of neutron and gamma radiation doses. In this study, we evaluated the neutron and gamma-ray doses in the thermal neutron irradiation field, which is necessary to investigate the effects of thermal neutrons on this semiconductor device.

EXPERIMENTS: The heavy water neutron irradiation facility (HWNIF) of KUR moderates the fast neutrons generated in the reactor core to thermal neutron energy using heavy water and aluminum. The HWNIF has a cadmium shutter behind the heavy water moderator to change the neutron energy. In addition, semiconductor devices are installed on substrates, and to observe semiconductor errors in real time, it is necessary to install a measurement device on a large carrier and irradiate it while acquiring data. Although changes in thermal neutron flux on a bismuth surface using rail device have been reported, no evaluation of neutron doses has been performed using a large carrier in combination with a collimator. Here, neutron and gamma-ray doses at the exit of the collimator with a collimator diameter of 300 mm x 300 mm were evaluated using the paired-ionization chamber method.

RESULTS: The figure 1 shows the neutron and gamma-ray dose results at the center of the collimator exit when the cadmium shutter aperture was varied. When the cadmium shutter is 0 mm, the dose rate was 190 mGy/hr/1 MW, with the majority of the dose coming from epithermal and fast neutrons. The gamma-ray dose also tends to increase with increasing thermal neutron flux due to the presence of secondary gamma rays generated by the collimator and other sources.

CONCLUSION: In the HWNIF, the relationship between cadmium shutter aperture and neutron and gamma -ray doses were derived in an irradiation field combining a large carrier and a collimator. Based on this information, irradiation of semiconductor devices will be carried out in the future.

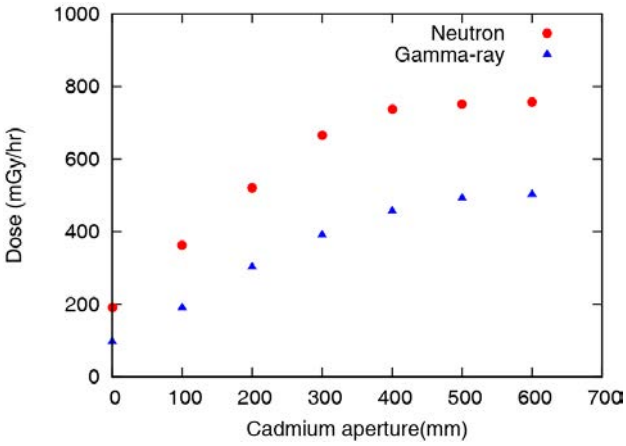

Fig. 1. Relationship between cadmium aperture and neutron and gamma-ray doses.

REFERENCES :

[1] Takashi Kato, Motonobu Tampo, Soshi Takeshita, Hiroki Tanaka, Hideya Matsuyama, Masanori Hashimoto, Yasuhiro Miyake, Muon-Induced Single-Event Upsets in 20-nm SRAMs: Comparative Characterization with Neutrons and Alpha Particles, IEEE Transactions on Nuclear Science, 68,1436-1444,2021.

PR6-16 Optimization of Bolus Shape for Boron Neutron Capture Therapy — Examination Using Simple Shaped Phantom for Experimental Verification —

T. Takata, M. Nojiri[1], A. Sasaki[1], Y. Sakurai, H. Tanaka and M. Suzuki

Institute for Integrated Radiation and Nuclear Science, Kyoto University
[1]Graduate School of Engineering, Kyoto University

INTRODUCTION: In Boron Neutron Capture Therapy (BNCT), an epithermal neutron beam has been utilized to penetrate a deep site of a patient's body based on its thermalization. However, thermal neutron buildup near a beam incident surface, associated with the use of epithermal neutron, causes dose deficiency in a case where a tumor extends to the vicinity of the patient surface. For such a case, a thermal neutron compensation bolus consisting of a hydrogen-rich material has been utilized to improve the dose distribution. In the present clinical BNCT, a bolus with a uniform thickness and a simple shape has been adopted. This study aims to increase the dose ratio of tumor to normal tissues more aggressively, by optimizing the bolus shape. An overview of the optimizing method was described in the previous report [1]. In addition, a verification using a water phantom has been attempted through experimental measurements [2]. As a part of the verification, the experiments using the phantom with/without a simple-shaped bolus were conducted before comparisons to the optimized one.

MATERIALS AND METHODS: A cylindrical water phantom with a height of 20 cm and diameter of 20 cm was used, assuming a head-and-neck case with a parotid gland cancer irradiated from the lateral direction. A spherical volume with a 4-cm diameter centered at a 2-cm depth from the side surface of the cylinder was defined as a planning target volume (PTV), assuming a tumor extended to a subcutaneous region. A tubular volume with a 3-cm diameter along the center axis of the cylinder was defined as an organ at risk (OAR), assuming a mucosal tissue of the oral cavity and pharynx [2].

The simple-shaped bolus was fabricated using a water bag with an acrylic container. The rectangular container with an outer dimension of 7.5 × 7.5 × 1.1 cm^3, filled with the water bag was attached to the beam incident surface (mid-height position of cylinder side) of the phantom (Figure 1).

In-phantom distributions of thermal neutron fluence with/without the bolus were measured using an activation method using gold wires. The gold wires were located in the phantoms to cover the PTV and OAR regions, and irradiated with the epithermal neutron beam of KUR Heavy Water Neutron Irradiation Facility (CO-0000F mode). After the irradiation, the gold wires were placed on an imaging plate (BAS-MS) to obtain the relative distributions of induced activities along the wires. Also, the absolute activities of some positions were determined by a well-type NaI(Tl) detector (SP-20, Ohyo Koken) or an HP-Ge detector to normalize the relative distribution obtained by the imaging plate.

RESULTS: Figure 2 shows the depth distributions of thermal neutron fluence along the beam axis for the cases with/without the rectangular bolus. In the case with the bolus, a shift in the distribution was observed toward the incident surface by the bolus thickness (1.1cm). The distributions along other wires, covering the PTV and OAR, will be derived in the same way. Also, the measurement with the optimized bolus will be conducted and analyzed to evaluate the improvement in volume-specific parameters of the thermal neutron fluence distribution.

ACKNOWLEDGMENT: This work was supported by JSPS KAKENHI Grant Number JP 17K17838. We thank Dr. Ken-ichi Tanaka of Kyoto Pharmaceutical University for allowing us to use the imaging plate reader with his helpful support.

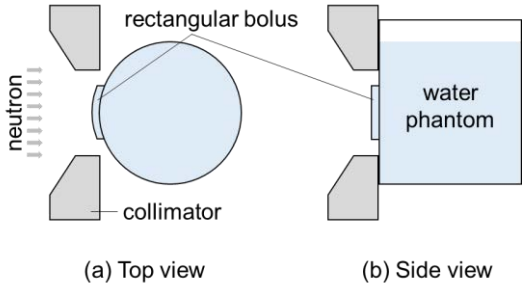

Fig. 1 Schematic layout of irradiation experiment using water phantom with rectangular bolus.

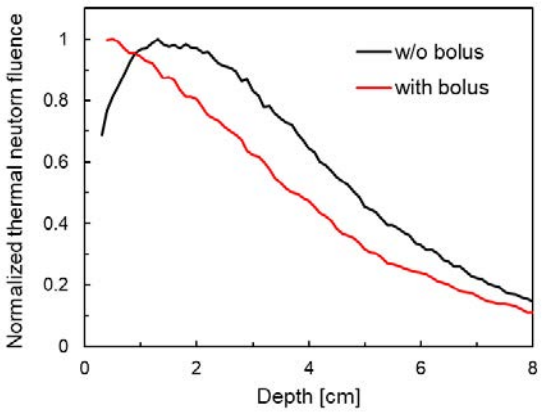

Fig. 2 Depth distributions of thermal neutron fluence for cases with/without bolus.

REFERENCES:

[1] T. Takata *et al.*, KURNS Progress Report 2019 (2020), 56.
[2] T. Takata *et al.*, KURNS Progress Report 2020 (2021), 83.

PR6-17 Annealing properties of boric acid infused PVA-GTA-I gel irradiated with neutrons

H. Yasuda[1], JE. Taño[1,2,3], CAB. Gonzales[1], Y. Sakurai[4]

[1]*Department of Radiation Biophysics, RIRBM, Hiroshima University*
[2] *Graduate School of Biomedical and Health Sciences, Hiroshima University*
[3] *Phoenix Leader Education Program for Renaissance from Radiation Disaster, Hiroshima University*
[4] *Institute for Integrated Radiation and Nuclear Science, Kyoto University (KURNS)*

INTRODUCTION: Since 2019, the authors have investigated the feasibility of infusing boric acid to an original radiochromic gel formula made of polyvinyl alcohol (PVA), glutaraldehyde (GTA), and iodide (I) [1,2], named "PGI gel" herewith. The results of the study demonstrated that addition of boric acid to the PGI gel worked to increase its sensitivity of response to neutron irradiation. We reported that the standard formula PGI gel was capable of reuse through annealing, that is, the irradiated gel samples were reverted by heating from red to clear with the initial absorbance values before irradiation [2]. In the present study, we tried to examine if the reversibility of PGI gels can be achieved with infusion of boric acid after a certain-period storage after irradiation with thermal neutron beams used for the boron neutron capture therapy.

EXPERIMENTS: All samples of PGI gel were prepared using ultrapure water and analytical grade chemicals purchased from FUJIFILM Wako Pure Chemical Corporation (Osaka, Japan). The standard formula of the PVA-GTA-I formula was infused with different boric acid concentrations of 0, 25 and 50 mM. The liquid mixtures were poured into PMMA cuvettes and stored inside a vacuum chamber (-0.08 MPa) for 3-hours. The cuvette samples were then covered with PE lids and stored inside a sterilizing oven at 50°C for 12 hours to convert from liquid to gel. The neutron irradiations of the samples were performed at the Heavy Water Neutron Irradiation Facility (HWNIF) of Kyoto University Reactor (KUR) with a 1MW nominal power. The samples were fixed on a rail system and irradiated at different periods: 20-, 40-, 80-, and 120-min. After irradiation, the samples were stored at room temperature and measured 55 days after irradiation. The optical absorbances were obtained using the NanoDrop OneC™ UV-Vis spectrometer (Thermo Fisher Scientific Inc., USA).
After the initial reading, the gel samples were annealed in the oven at 50°C at time intervals of 24, 48, 72, and 96 hours. It should be noted that after each annealing time interval, the samples were stabilized at room temperature for 2 hours before measurement.

RESULTS: Good linearities were confirmed in the dose responses of the PGI gels having different boron concentrations. While, different levels of natural oxidation were observed among the different formula gels after a certain storage period (~55 days). As to the effects of annealing process at 50°C, it was found that the PGI gels infused with boric acid needed longer time to become clear than the standard one. Also, the time for completely erasing the radiation-induced color tended to be longer in the samples with higher boric acid concentration.
The time changes of decolorization process were well approximated with an exponential function below for all the cases:

$$A(t) = A_0 \times e^{-\lambda \cdot t} \quad (1)$$

where $A(t)$ is the absorbance of a PGI gel at the wavelength of 490 nm at the annealing time t; A_0 is initial absorbance ($=A(0)$); and λ is an empirically determined parameter indicating the speed of color decay. The estimated values of A_0 and λ are shown in Fig.1 as function of the time of neutron irradiation. Notable dependence of those fitting parameter values on boric acid concentration were seen. These findings imply that addition of boric acid can improve the sensitivity of the PGI gel but lower the practicality as it makes longer the annealing time. Further investigation to confirm the reusability is to be continued.

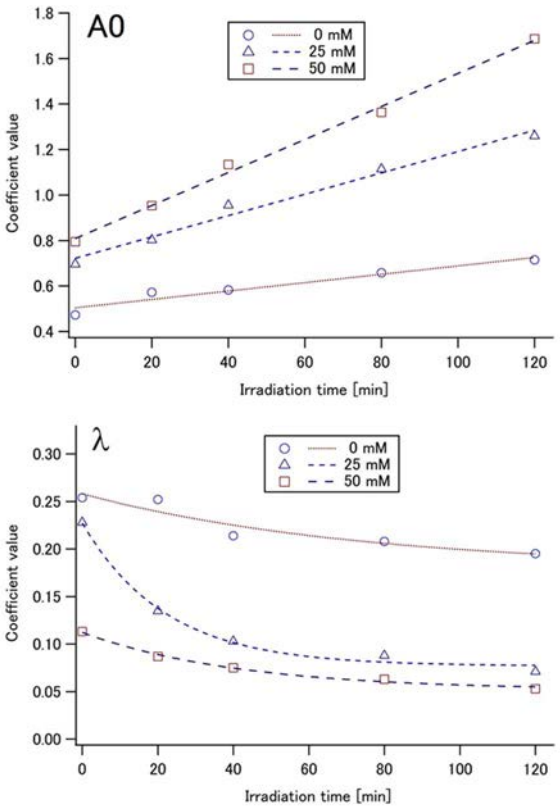

Fig. 1 The estimated parameter values: A_0 (above) and λ (below) obtained through fitting with eq.1 as function of neutron irradiation time for the PGI cells with different boric acid concentrations.

REFERENCES:
[1] Taño JE *et al.* 2020. *Radiat Meas.* **134** 106311.
[2] Taño JE *et al.* 2021. *Radiat Meas.* **149** 106674.

PR6-18 Three dimentional model for pre-clinical assessments in BNCT

K.Igawa, [1]A.Sasaki, [2]K.Izumi, [2] E.Naito, [3]M.Suzuki, [3]N.Kondo, [3] Y.Sakurai

Neutron Therapy Research Center, Okayama University

[1]Department of Oral Maxillofacial Surgery, Okayama University

[2]Graduate School of Medical and Dental Sciences Oral Life, Niigata University

[3]Institute for Integrated Radiation and Nuclear Science, Kyoto University

INTRODUCTION: In Boron Neutron Capture Therapy (BNCT), the Boron dose and neutron dose in tumor cells are the key factors. The development of boron agents for BNCT requires the evaluation system bridging the gap between in vivo and in vitro research. Also, from the viewpoint of the guiding principles for animal experiments (3Rs:Replacement, Reduction and Refinement), the alternative research methods that do not use animals, are required for BNCT. On the other hand, three-dimensional (3D) models have been widely used in cancer research due to their ability to mimic multiple features of the tumor microenvironment [1]. Therefore, the validity of the 3D in vitro oral cancer model for pre-clinical investigations in BNCT is examined in this study.

EXPERIMENTS: First, we fabricated 3D in vitro oral cancer and normal oral mucosa models. For the facilitation of 3D in vitro oral cancer model, normal oral mucosa fibroblasts（Niigata University ） were embedded and cultured in type I collagen matrix (Niita-gelatin, Japan) for 7 days under a humidified atmosphere of 5% CO_2 at 37 ◦C. Oral squamous carcinoma cells（HSC3, Riken Cell Bank） were seeded on top of the surface of 3D collagen matrix, and then, the composite was cultured under a submerged condition for additional 7 days in DMEM medium (Wako, Japan) supplemented with 10 % fetal bovine serum (Sigma -Aldrich, USA) and 100 unit/ml penicillin and 100 µg/ml streptomycin (1% p/s) (Thermo Fisher Scientific, USA) (Fig.1) [2]. Similarly, the 3D normal oral mucosa model was manufactured by seeding normal oral keratinocyte (Niigata University) on the top of the collagen matrix with normal oral fibroblasts using complete EpiLife® medium containing 0.06 mM Ca^{2+} [3]. The fabrication of both models was completed by culturing at an air-liquid interface for another 7 days (total 21 days in culture). After the infusion of Boron (Steboronine®, Stella pharma, Japan) or Phosphate Buffered Saline (PBS, Sigma -Aldrich, USA), 3D in vitro models were incubated for 2 hours, washed by PBS, and irradiated by neutron for 20 minutes. After irradiation, they were cultured for another 7 days (Fig. 2). Finally, the 3D models were fixed with 10 % formalin, embedded in paraffin, cut in 5 µm sections and stained with hematoxylin and eosin.

RESULTS: The histological examinations of the 3D oral cancer model after neutron irradiation revealed that the cancer cell layer appeared to be apoptotic after neutron irradiation. More remarkably, the thickness of the underlying fibroblasts-embedded collagen matrix was significantly thinner in BNCT group, compared with control group as shown in Fig.3(a). In contrast, in the normal oral mucosa model, the epithelial layer did not seem to be different after neutron irradiation, except moderate irregular cellular arrangement of the basal cells layer. (Fig.3b). Additionally, the thickness of the underlying collagen matrix did not change after neutron irradiation. These results suggest that our 3D in vitro models could be useful to evaluate cellular response to BNCT for oral cancer cells as well as the surrounding normal oral mucosa, and would be an alternative tool to animal test for BNCT.

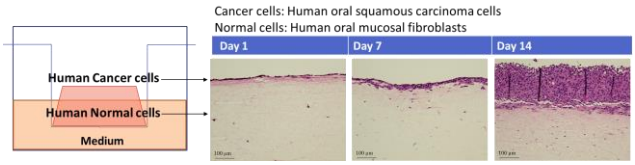

Fig.1. Diagram of manufacturing 3D oral cancer model

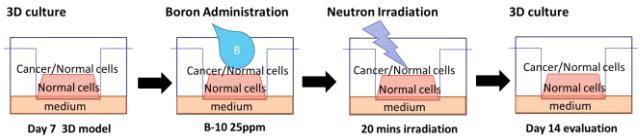

Fig.2. BNCT protocol for 3D in vitro models

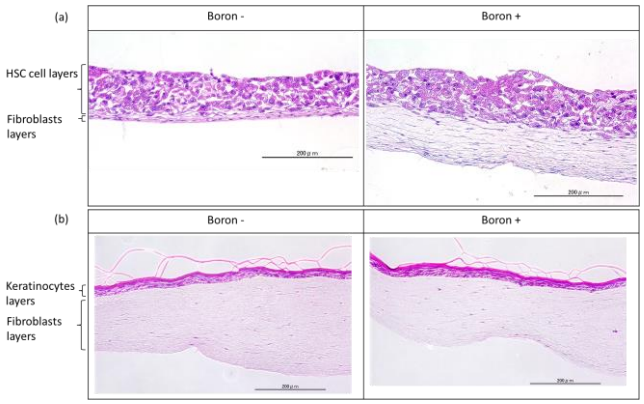

Fig.3. Histology of the 3D cancer model at 7 days after neutron irradiation. (a) 3D oral cancer model (b) 3D normal oral mucosa model.

REFERENCES:

[1] D Corallo *et al.*, frontiers in Immunology vol.11 (2020) https://doi.org/10.3389/fimmu.2020.584214.
[2] K Haga *et al.,* Translational Oncology 12 (2021) DOI: 10.1016/j.tranon.2021.101236.
[3] A Uenoyama *et al.*, Biosci, Biotechnol, and Biochem, 80（2016）DOI:10.1080/09168451.2016.1153957.